

Measurement and Control of Ionization Waves of Arbitrary Velocity in the Quasi-Far Field

P. Franke,^{1,2} D. Turnbull,¹ J. Katz,¹ J. P. Palastro,¹ I. A. Begishev,¹ J. Bromage,^{1,3} J. L. Shaw,¹ R. Boni,¹ and D. H. Froula^{1,2}

¹Laboratory for Laser Energetics, University of Rochester

²Department of Physics & Astronomy, University of Rochester

³Institute of Optics, University of Rochester

Ionization fronts with precisely controlled characteristics could help to overcome fundamental limitations in laser-plasma-based photonics applications by improving phase matching, extending interaction lengths, and facilitating better control of plasma conditions. These capabilities are particularly useful in plasma-based light manipulation processes such as photon acceleration,^{1–6} Raman amplification,^{7–12} and THz generation^{13–15}—processes that could lead to a new generation of exotic, compact, and versatile radiation sources.

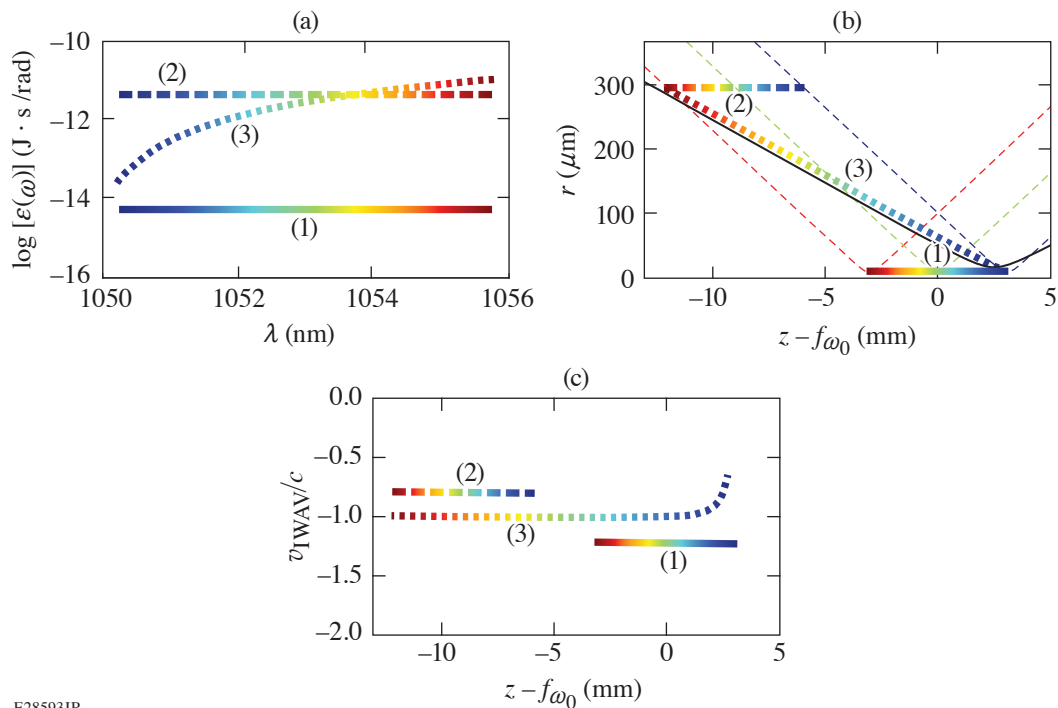
Highly controllable ionization fronts can be driven using a recently developed method called the “flying focus,” in which a chirped laser pulse is focused by a hyperchromatic optic such as a diffractive lens.^{16,17} The chromatic aberration causes different frequencies in the laser pulse to come to focus at different positions along the propagation axis. For a fixed focal geometry, the temporal delay between when each frequency reaches its focal position is determined by the chirp, which can be adjusted to cause the point of the maximum laser intensity to move at any velocity over distances that can greatly exceed the Rayleigh length.

When the instantaneous intensity of a flying-focus pulse exceeds the ionization intensity threshold (I_i) of a background gas an ionization front is produced that tracks the propagation of an intensity isosurface at I_i (Ref. 18). These ionization waves of arbitrary velocity (IWAV’s) were experimentally demonstrated to have predictable and easily adjustable velocities equal to the expected flying-focus velocity when driven by a laser pulse with a highly uniform power spectrum in the laser far field.¹⁹

While modification of the power spectrum was proposed as a means to increase control of IWAV propagation,¹⁸ previous theoretical and experimental investigations were limited to the laser far field and mainly considered flat power spectra, i.e., high-order super-Gaussians. In this parameter regime, all frequencies in the bandwidth have just enough power to ionize near their minimum spot size. Experimental observation of channels formed by IWAV propagation indicated radii $\sim 10 \mu\text{m}$, close to the measured far-field laser spot size. Such small-diameter IWAV’s would have limited usefulness in applications because of the difficulty of coupling another beam into the IWAV, the small available cross section for interaction, and strong refraction resulting from the short transverse density scale lengths.

It is possible to increase the diffraction-limited minimum spot size by increasing the f number so that larger IWAV’s can be driven in the laser far field. It may be experimentally favorable, however, to simply increase the total pulse power so that all wavelengths ionize before they reach their minimum spot size. Operation in this so called quasi-far-field (QFF) regime, where the transverse extent of the laser field is large compared to its diffraction-limited spot size, provides control of the IWAV radius without changing the focusing geometry. Furthermore, it offers the possibility of using nonuniform power spectra to control the dynamic behavior of the IWAV’s. QFF IWAV’s may be the only path forward for applications that require a significant pump intensity to exist behind the ionization front, such as flying-focus-driven plasma Raman amplification.^{7,8}

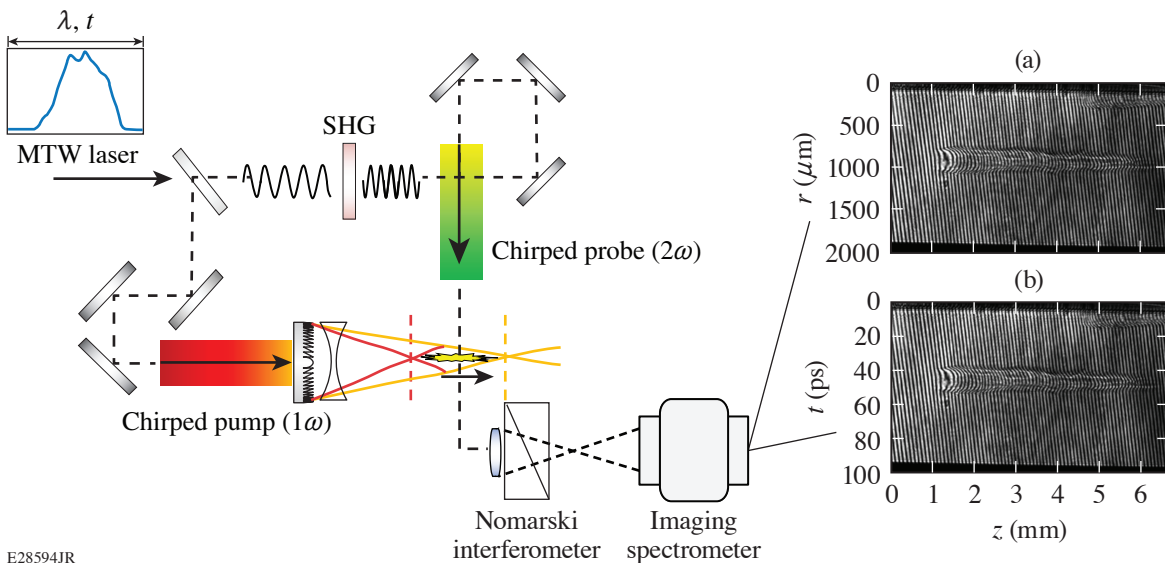
This research presents the first experimental demonstration of IWAV’s in the QFF and develops a new theory to predict their behavior. Figure 1 describes a simple model of IWAV propagation when the flying-focus power spectrum is nonuniform and uses it to develop an intuitive understanding of QFF IWAV’s and demonstrate enhanced control of IWAV characteristics through spectral shaping. Figure 2



E28593JR

Figure 1

(a) Calculations of the IWAV (b) radius and (c) velocity are shown for the spectral energy densities. Cases (1) and (2) show the simple far-field and QFF IWAV propagations, respectively. Case (3) shows that the spectrum can be adjusted to change the IWAV radius and match the f number of a separate beam [black line in (b)], but still maintain a constant velocity. Case (3) also shows that the IWAV range can be increased beyond the already-extended focal region and that the IWAV can be accelerated through spectral shaping. (b) Single-frequency radii for the edges (blue and red) and center (green) of the bandwidth are shown as single-color dashed lines. (c) Velocities for cases (1) and (2) are shown offset from $v_{\text{IWAV}} = -c$ by $\sim 20\%$ for clarity, but all calculations were done for $v_{\text{IWAV}} = -c$.



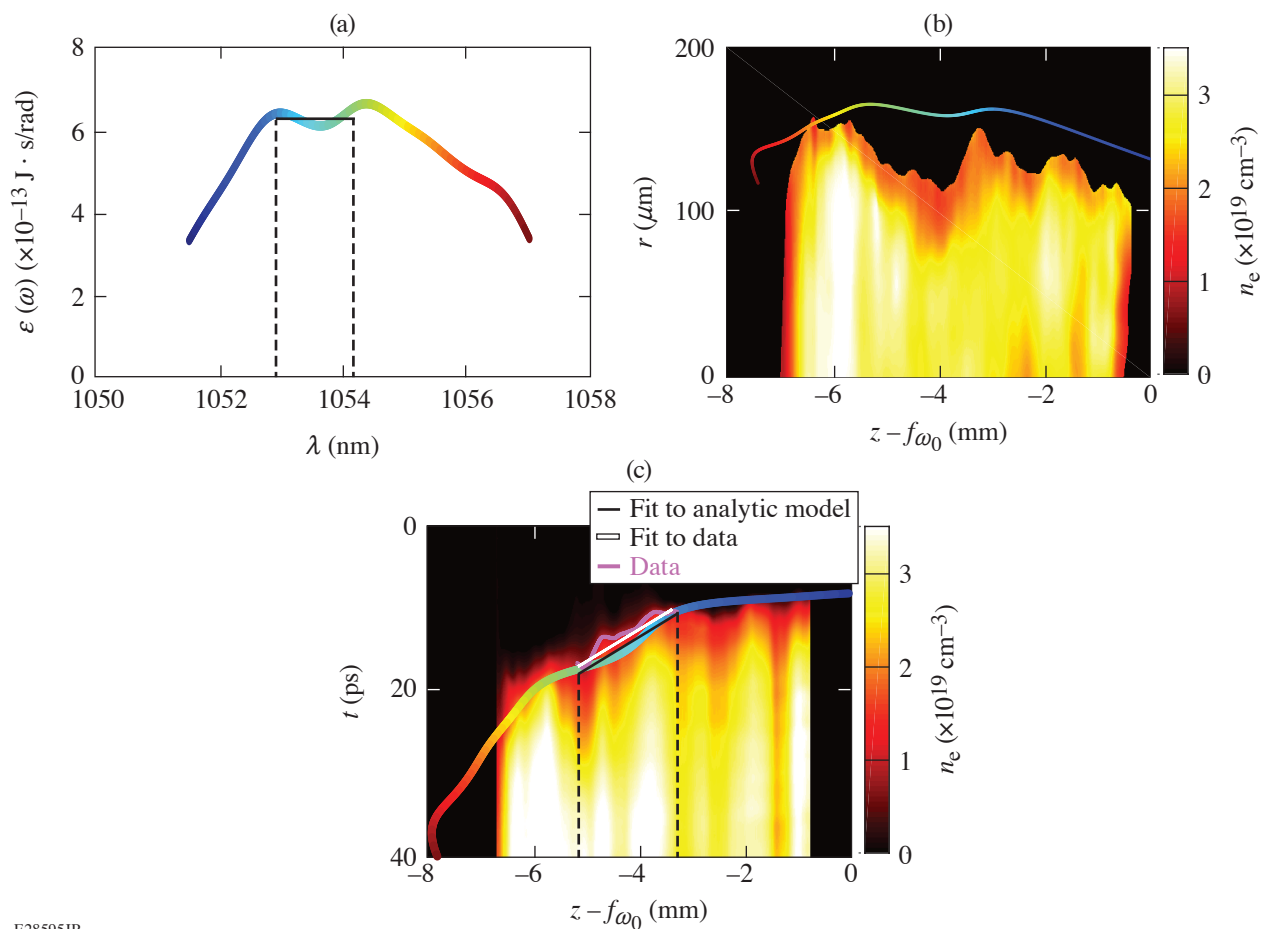
E28594JR

Figure 2

The Multi-Terawatt (MTW) laser was split into a 1ω pump beam that drove IWAV's in a hydrogen gas jet and a 2ω probe beam that passed through the interaction region perpendicular to the IWAV propagation with variable timing, allowing (a) conventional 2-D and (b) 1-D spectrally resolved interferograms of the IWAV propagation to be collected. The 2-D data allow for the reconstruction of the electron density as a function of radial and axial distance late in time. The 1-D and 2-D data together allow extraction of the electron density as a function of time and axial distance along the pump beam propagation axis while the IWAV is propagating through the interaction region.

describes an experimental setup that incorporates a novel spectrally resolved interferometry diagnostic that allows for the inference of IWAV characteristics such as velocity, radius, and temporal density scale length. Experimental results are compared to the theory developed in this research (Fig. 3). IWAV's with radii $\sim 10\times$ larger than previously observed are experimentally demonstrated. The new theory accurately predicts the observed data, even when the direct correspondence to the flying-focus theory is invalid, but obtain consistency between all theories and the data in general. The experimental ionization rates are compared to a computational model described in Ref. 18 and obtain agreement (Fig. 4), which lends experimental validation to recent predictions of the extreme frequency upshifts achievable by co-propagating a witness laser pulse with a flying-focus-driven IWAV.

This material is based upon work supported by the Department of Energy National Nuclear Security Administration under Award Number DE-NA0003856, the Fusion Energy Science under Award Numbers DE-SC0019135, DE-SC0016253, the University of Rochester, and the New York State Energy Research and Development Authority.



E28595JR

Figure 3

(a) The experimental spectral energy density was used to calculate an expected radial profile and trajectory [multicolor curves in (b) and (c), respectively], which are overlaid on the electron density data extracted from 2-D interferometry and spectrally resolved interferometry [color bar in (b) and (c), respectively]. The predicted radial profile and trajectory are in agreement with the data over the entire bandwidth. A “flat” region of the spectrum and the trajectory that corresponds to this part of the spectrum is demarcated by vertical dashed black lines in (a) and (c). In this region, the flying-focus velocity ($-0.75c$), the predicted IWAV velocity ($-0.73c$), and the measured velocity ($-0.71c$) are all in agreement.

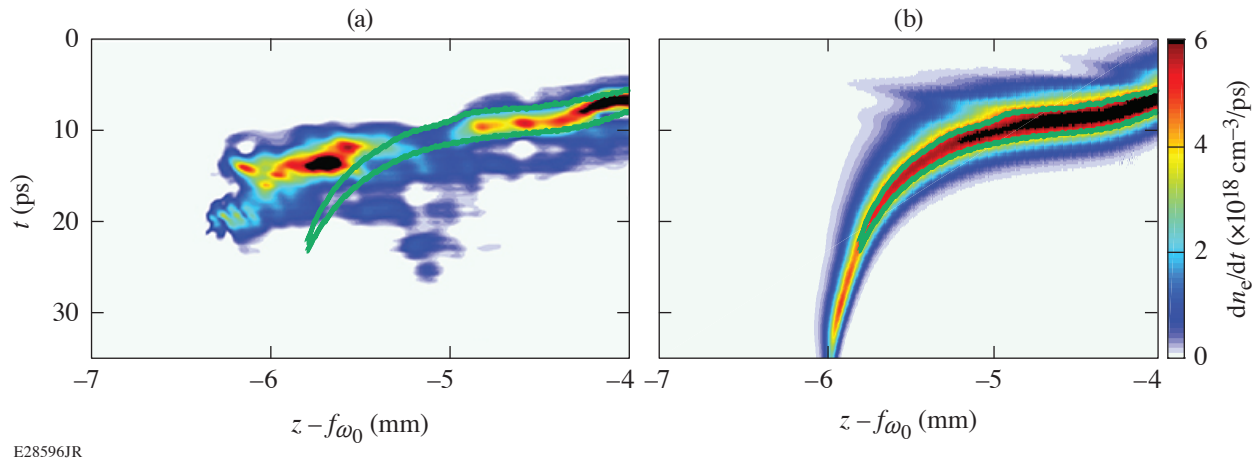


Figure 4

(a) The measured temporal density gradient (ionization rate) has values and a trajectory that are close to those predicted by simulations of ionization as a result of (b) flying-focus pulse propagation. An outline of the simulated data is shown in both (a) and (b) as a green curve.

1. A. Howard *et al.*, "Photon Acceleration in a Flying Focus," to be published in Physical Review Letters.
2. S. C. Wilks *et al.*, Phys. Rev. Lett. **62**, 2600 (1989).
3. J. T. Mendonça, *Theory of Photon Acceleration*, Series in Plasma Physics (Institute of Physics Publishing, Bristol, England, 2001).
4. J. M. Dias *et al.*, Phys. Rev. E **66**, 056406 (2002).
5. N. C. Lopes *et al.*, Europhys. Lett. **66**, 371 (2004).
6. L. Oliveria e Silva and J. T. Mendonca, IEEE Trans. Plasma Sci. **24**, 316 (1996).
7. D. Turnbull *et al.*, Phys. Rev. Lett. **120**, 024801 (2018).
8. D. Turnbull *et al.*, Plasma Phys. Control. Fusion **61**, 014022 (2019).
9. V. M. Malkin, G. Shvets, and N. J. Fisch, Phys. Rev. Lett. **82**, 4448 (1999).
10. V. M. Malkin, G. Shvets, and N. J. Fisch, Phys. Rev. Lett. **84**, 1208 (2000).
11. Y. Ping *et al.*, Phys. Rev. Lett. **92**, 175007 (2004).
12. Y. Ping *et al.*, Phys. Plasmas **16**, 123113 (2009).
13. K. Y. Kim *et al.*, Opt. Express **15**, 4577 (2007).
14. P. Sprangle *et al.*, Phys. Rev. E **69**, 066415 (2004).
15. C. D'Amico *et al.*, Phys. Rev. Lett. **98**, 235002 (2007).
16. D. H. Froula *et al.*, Nat. Photonics **12**, 262 (2018).
17. A. Sainte-Marie, O. Gobert, and F. Quéré, Optica **4**, 1298 (2017).
18. J. P. Palastro *et al.*, Phys. Rev. A **97**, 033835 (2018).
19. D. Turnbull *et al.*, Phys. Rev. Lett. **120**, 225001 (2018).